HAL
open science

Neutron Diffraction Investigation of the DyFe11Ti Magnetic Structure and Its Spin Reorientations

Olivier Isnard, Eder Kinast

To cite this version:

Olivier Isnard, Eder Kinast. Neutron Diffraction Investigation of the DyFe11Ti Magnetic Structure and Its Spin Reorientations. Engineering, 2020, 6 (2), pp.154-158. 10.1016/j.eng.2019.11.009 . hal-04099870

HAL Id: hal-04099870

https://hal.science/hal-04099870v1

Submitted on 26 May 2023

HAL is a multi-disciplinary open access archive for the deposit and dissemination of scientific research documents, whether they are published or not. The documents may come from teaching and research institutions in France or abroad, or from public or private research centers.

L'archive ouverte pluridisciplinaire **HAL**, est destinée au dépôt et à la diffusion de documents scientifiques de niveau recherche, publiés ou non, émanant des établissements d'enseignement et de recherche français ou étrangers, des laboratoires publics ou privés.

Engineering 6 (2020) 154–158

Contents lists available at ScienceDirect

Engineering

journal homepage: www.elsevier.com/locate/eng

Research
Rare Earth Permanent Magnets—Article

Neutron Diffraction Investigation of the $DyFe_{11}Ti$ Magnetic Structure and Its Spin Reorientations

Olivier Isnard [a,*], Eder J. Kinast [b]

[a] University Grenoble Alpes, Institut Néel du CNRS, 25 rue des Martyrs, Grenoble 38042, France
[b] Universidade Estadual do Rio Grande do Sul, Porto Alegre, RS 90010-191, Brazil

ARTICLE INFO

Article history:
Received 23 July 2018
Revised 3 February 2019
Accepted 11 March 2019
Available online 22 November 2019

Keywords:
Neutron diffraction
Magnetic phase diagram
Crystal structure

ABSTRACT

In this article, we report on the magnetic structure of $DyFe_{11}Ti$ and its thermal evolution as probed by neutron powder diffraction. A thermodiffraction technique was used to follow the temperature dependence of the magnetic moments, as well as their orientation. The Dy and Fe moments were coupled to each other in an antiparallel manner to form a ferrimagnet, where the easy magnetization direction at 2 K was the [110] axis in the basal (*a*, *b*) plane. This magnetic structure underwent two successive spin reorientation phenomena with increasing temperature. A large Dy magnetic moment of 9.7 Bohr magneton (μ_B) was obtained at low temperatures, and the magnitude decreased rapidly to 7.5μ_B at 200 K. The largest Fe magnetic moment was observed on the Fe 8*i* position. A $ThMn_{12}$-type crystal structure was preserved in the studied temperature range, despite the large changes of the magnetic structure. A sharp tilt was observed at the first-order spin reorientation, T_{SR1}; the angle between the easy magnetization axis and the crystal *c* axis was reduced from 90° at 2 K to about 20° at 200 K (where *c* is the easy axis above 200 K); and the Dy and Fe magnetic moments maintained an antiparallel coupling.

© 2020 THE AUTHORS. Published by Elsevier LTD on behalf of Chinese Academy of Engineering and Higher Education Press Limited Company This is an open access article under the CC BY-NC-ND license (http://creativecommons.org/licenses/by-nc-nd/4.0/).

1. Introduction

The investigation of iron (Fe)-rich intermetallic compounds containing rare-earth metals (R) has attracted considerable interest during the last three decades, due to the potential of these compounds to act as hard magnetic materials. These remarkable materials can potentially combine a high ordering temperature and high magnetization with significant magnetocrystalline anisotropy and coercivity. In addition to their potential for application, R–Fe intermetallic compounds offer researchers the opportunity to perform extensive fundamental studies of the magnetic behavior of itinerant 3d electrons and localized 4f electronic states. Several studies have investigated the unusual behavior of $RFe_{12-x}M_x$ intermetallic compounds [1–3]. Firstly, no RFe_{12} compound has been reported as a bulk sample; secondly, the use of a stabilizing element, M, is necessary in order to obtain the $RFe_{12-x}M_x$ phase and observe a $ThMn_{12}$ structure type. When M = Ti, a relatively high Curie temperature can be obtained for these phases, and can be further improved by the insertion of a light element within the crystal lattice, such as hydrogen (H), carbon (C), or nitrogen (N) [4,5]. These materials are also of interest due to their relatively complex magnetic phase diagram when the R and Fe sub-lattices have different preferential anisotropy directions [1,2,4].

The $ThMn_{12}$ structure, which was originally determined by Florio et al. [6], is closely related to the $CaCu_5$ structure type by an ordered substitution of a rare-earth element by a pair of 3d transition metals following the relation $2RM_5 - R + 2M \rightarrow RM_{12}$. Half of the R atoms are consequently replaced by M atoms at the 8*i* position. This substitution results in a change of crystal symmetry, and the tetragonal *I4/mmm* space group is retained. In addition to the 2*a* position occupied by the rare-earth element, transition metal atoms are observed on three inequivalent atomic positions: 8*i*, 8*j*, and 8*f* [1,7,8]. The $ThMn_{12}$ structure is also related to the parent Th_2Ni_{17} structure. For a detailed description of the relationships between these structures, the reader is referred to the work of Hu et al. [8].

This article focuses on the magnetic structure of $DyFe_{11}Ti$ compounds and on its temperature dependence. This compound has attracted a great deal of research interest due to its original magnetic behavior and the presence of two spin reorientation transitions. At room temperature, $DyFe_{11}Ti$ exhibits a uniaxial

* Corresponding author.
E-mail address: olivier.isnard@neel.cnrs.fr (O. Isnard).

https://doi.org/10.1016/j.eng.2019.11.009
2095-8099/© 2020 THE AUTHORS. Published by Elsevier LTD on behalf of Chinese Academy of Engineering and Higher Education Press Limited Company
This is an open access article under the CC BY-NC-ND license (http://creativecommons.org/licenses/by-nc-nd/4.0/).

alignment of the magnetic moments along the *c* axis, as has been derived from single-crystal studies and from Mössbauer spectroscopy [9–12]. The low-temperature behavior is more complex, and has been the subject of several magnetic studies. Contradicting conclusions were drawn from the studies of different sets of single crystals [9–14], particularly in regards to the first- or second-order nature of the lowest temperature spin reorientation, T_{SR1}. However, those researchers agreed that T_{SR2}, the spin reorientation above 200 K, is of the second order. Nevertheless, no direct investigation of the magnetic structure by neutron diffraction has been reported to date. This is the purpose of the present study, which focuses on the low-temperature magnetic behavior around T_{SR1} with the aim of shedding new light on the complex magnetic phase diagram of $DyFe_{11}Ti$.

2. Material and methods

The sample preparation was performed by means of high-frequency induction melting in a purified argon (Ar) atmosphere, starting from the pure elements. To homogenize the obtained ingot, annealing was performed in an evacuated quartz ampoule for ten days at 950 °C. Sample purity was investigated using X-ray diffraction and thermomagnetic measurements. Neutron diffraction measurements were performed on D1B, a powder diffractometer operated by the French National Center for Scientific Research (CNRS) as a Collaborative Research Group at Institut Laue-Langevin (ILL), in Grenoble, France. A wavelength of 2.52 Å was selected by a pyrolytic graphite monochromator. We used a multicounter containing 400 cells, with a step of 0.2° between neighboring cells; the detector covered a 2θ angular range of 80°. The detector was set at an initial position of 2θ = 20°, since no Bragg reflection was observed at a lower angle. The diffractograms were taken at different temperatures ranging from 1.5 to 202 K. The crystal structure and magnetic parameters were refined using the Rietveld method implemented in the FullProf program [15]. The definition of the agreement factors is given in the corresponding FullProf program manual. In order to minimize neutron absorption by the dysprosium (Dy) nucleus, we used a special annular sample holder.

3. Results and discussion

Rietveld refinement of the neutron data revealed the presence of elemental iron as a minority phase in the studied compound (its content was below 1%). Neutron diffraction also indicated the presence of traces of $TiFe_2$ as impurity. A plot of the refinement of the diffraction pattern recorded at 2 K for $DyFe_{11}Ti$ is given in Fig. 1. Thanks to the large contrast between the atomic neutron coherent scattering length of the titanium (Ti) and Fe nuclei, the Ti atom location and content could be precisely determined. As shown in Table 1, the Ti atoms were located exclusively on the 8*i* position of the $ThMn_{12}$ structure type, whereas the Fe atoms were found on the remaining transition metal positions 8*i*, 8*j*, and 8*f*. This preferential location on the 8*i* site is in line with earlier reported results on isotype $RFe_{11}Ti$ intermetallics [7], and is attributed to the larger volume of the 8*i* position. The refined Ti content was in excellent agreement with the initial $DyFe_{11}Ti$ stoichiometry, confirming the very low content of "Ti-containing impurity." An analysis of the magnetic contribution to the neutron diffraction pattern indicated that the Dy and Fe magnetic moments were coupled anti-ferromagnetically and were lying within the basal (*a*, *b*) plane, forming a 90° angle with the *c* axis. Due to the contradicting results on the orientation of the magnetic moments [9,13], two directions were tested: [100] and [110]. Rietveld refinement at 2 K gave a significantly better fit when the magnetic

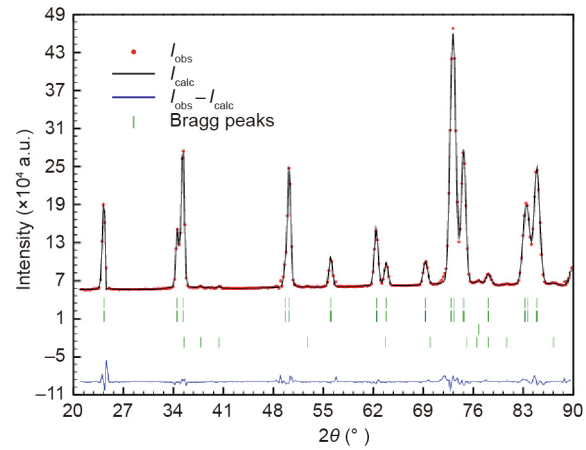

Fig. 1. Plot of the Rietveld refinement of the neutron diffraction pattern recorded at 2 K for $DyFe_{11}Ti$. The red points are experimental data and the black curve corresponds to Rietveld fit. The first and second rows of green Bragg peaks refer to the nuclear and magnetic contribution, respectively. The third and fourth rows refer to the Bragg peak position of the traces (< 1%) of alpha Fe and $TiFe_2$, respectively, as impurities. A.u.: arbitrary units; I_{obs}: ovserved intensity; I_{calc}: calculated intensity.

moments were along the [110] direction—a result that agrees with Refs. [13,14]; consequently, the easy magnetization axis is [110]. At 2 K, the magnetic moment carried by the Dy atoms, 9.7 Bohr magneton (μ_B), was very close to the $10\mu_B$ that was expected from the trivalent state. The Fe magnetic moment was found to be aligned ferromagnetically and to have different values for the three inequivalent Fe atomic positions; the largest moment was observed on the Fe 8*i* site, whereas the smallest was found on the 8*f* site. The large magnetic moment observed on the 8*i* position is a general feature of the $RFe_{12-x}M_x$ compounds, and has been suggested to result from both the large atomic volume and the possible presence of a significant orbital contribution to the Fe magnetic moment [16]. Such a sequence of Fe magnetic moments—that is, 8*i* > 8*j* > 8*f*—is in good agreement with the hyperfine field derived for the three Fe positions in $RFe_{11}Ti$ isotype compounds [17,18]. No magnetic moment was refined on the Ti atoms. This does not exclude the possibility of a weak moment due to polarization by the surrounding Fe and Dy atoms on titanium. However, such a weak moment is likely to be below the sensitivity of the powder neutron diffraction used in this work.

In order to investigate the evolution of the magnetic structure of $DyFe_{11}Ti$, diffraction patterns were recorded every 2.5 K during heating from 1.5 to 202 K. A zoom of the low-angle part (between 21° and 41° in 2θ) is plotted in Fig. 2, highlighting the main changes in diffraction intensities. This plot corresponds to the (110), (200), and (101) Bragg peaks, which were observed at 24°, 34°, and 35°, respectively. Whereas the first two peaks showed an increase in intensity, the (101) presented the opposite behavior, with a rapidly decreasing intensity when approaching 100 K. Such behavior at low temperature is indicative of a spin reorientation of the magnetic moments, and motivated our further investigation. The presence of a magnetic contribution appearing at high temperature for the (110) and (200) peaks indicates the appearance of a magnetic moment component perpendicular to the scattering vector. Each of the 86 neutron diffraction patterns were refined in order to obtain the temperature dependence of the magnetic structure. The easy magnetization axis was [110] below T_{SR1}. Up to about 89 K, the best fit was obtained by keeping a 90° angle between the Dy and Fe magnetic moments on the one hand, and the *c* axis on the other hand. Such easy plane orientation is in good agreement with the earlier reported ^{57}Fe Mössbauer spectroscopy results [12,17]. Above 91 K and up to 202 K, the diffraction patterns

Table 1
Crystal structure parameters as deduced from Rietveld refinement of the neutron powder diffraction data recorded for $DyFe_{11}Ti$ at 2 K.

Atom	Site	x/a	y/b	z/c	Occupancy (%)	$M_{[110]}(\mu_B)$
Dy	2*a*	0	0	0	100	−9.7(2)
Fe	8*f*	0.25	0.25	0.25	100	1.8(1)
Fe	8*j*	0.2759(8)	0.5	0	100	2.1(1)
Fe/Ti	8*i*	0.355(1)	0	0	78/22(2)	2.2(1)

$a = b = 8.4826$ Å, $c = 4.7682(3)$ Å. x, y, and z are the atomic position parameters. The agreement factors are as follows: $R_p = 1.7\%$, $R_B = 1.1\%$, and $R_{Mag} = 1.15\%$. $M_{[110]}$: magnetic moment along [110] direction.

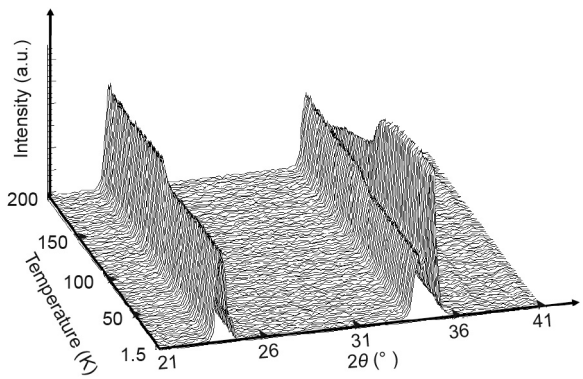

Fig. 2. Temperature dependence of a low-angle portion of the neutron powder diffraction pattern recorded between 1.5 and 200 K for $DyFe_{11}Ti$. The observed evolution reflects the occurrence of a spin reorientation transition upon temperature change.

were fitted by refining the angle between the *c* axis and the magnetization direction. This gave significantly better refinement results. An example of the refinement is plotted for the 200 K pattern in Fig. 3. It is worth noting that the Dy magnetic moment experienced a large reduction of more than $2\mu_B$ from 2 to 200 K. This finding confirms the strong temperature dependence of the 4f electron magnetic moments. The Fe magnetic moments are much less sensitive to temperature changes, and were reduced by only $0.2\mu_B$ per Fe atom in this temperature range. This result can be attributed to the rather high ordering temperature of $DyFe_{11}Ti$—that is, 552 K [12]—which led to a saturated state of Fe moments below 200 K.

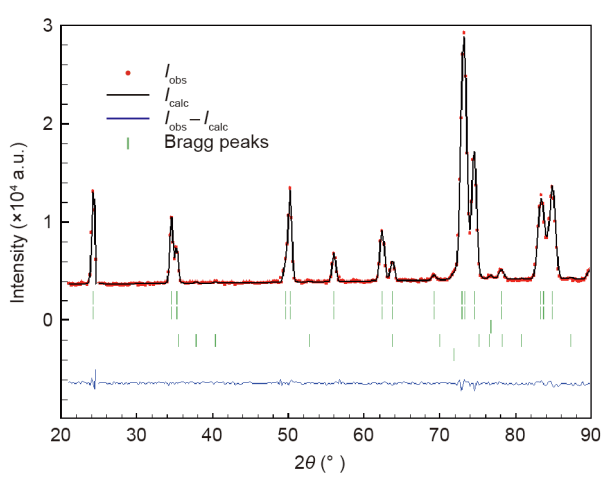

Fig. 3. Plot of the Rietveld refinement of the neutron diffraction pattern recorded at 200 K for $DyFe_{11}Ti$. The red points are experimental data and the black curve corresponds to Rietveld fit. The first and second rows of Bragg peaks refer to the nuclear and magnetic contribution, respectively. The third and fourth rows refer to the Bragg peak position of the traces (< 1%) of alpha Fe and $TiFe_2$, respectively, as impurities. The last row is the contribution of the vanadium tail of the cryostat.

The results of the Rietveld analysis of the thermodiffraction data are given in Figs. 4–6. Table 2 presents the structural and magnetic data obtained from Rietveld refinement of the pattern recorded for $DyFe_{11}Ti$ at 200 K. As derived from neutron diffraction, the thermal evolution of the angle between the easy magnetization direction and the *c* axis indicated that $DyFe_{11}Ti$ exhibits an easy plane anisotropy below 90 K, whereas an easy axis has been reported at 240 and 300 K from ^{57}Fe Mössbauer spectroscopy [12]. As shown in Fig. 4, the first spin reorientation occurring at $T_{SR1} = 90$ K is sharp and manifests itself by a sudden drop of the angle from 90° to 72° for 89 and 93 K, respectively. This angle then decreases much more slowly above 105 K. A smooth decrease is observed from 50° to 30°, followed by a slightly more pronounced decrease when approaching the second spin reorientation, T_{SR2}, whose value is above 200 K.

In his theoretical study, Kuz'min [13] demonstrated that spatial inhomogeneities of the sample composition (e.g., Ti content) play an important role in the magnetic behavior and gradual character of the first-order spin reorientation in $DyFe_{11}Ti$. The present neutron diffraction investigation performed on a sample with defined stoichiometry provides a clear picture of the magnetic phase diagram and the spin reorientation phenomenon observed on $DyFe_{11}Ti$. The temperature dependence of the angle of rotation of the magnetization, as derived from neutron diffraction, is similar to that reported in Ref. [19]. Indeed, a rapid tilt of the easy magnetization direction to the plane can be observed for $T < T_{SR1}$ in Fig. 4. The main differences are the onset temperature value of this spin reorientation (T_{SR1} 50 K against 90 K here) and the value of the angle plateau above this spin reorientation (40° against 50° in our case). These changes probably arise from the different Ti concentrations, as has been discussed elsewhere [13]. This interpretation is supported by the significant difference between the ordering temperature of 530 K for the single crystal investigated

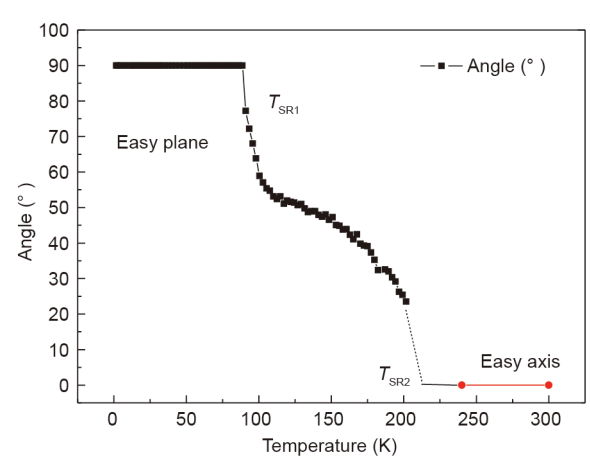

Fig. 4. Thermal evolution of the tilt angle between the easy magnetization direction and the *c* crystal axis as derived from the Rietveld refinement of the neutron powder diffraction patterns recorded for $DyFe_{11}Ti$. The circles refer to the Mössbauer data on the same sample [12], and the dotted line is a visual guide.

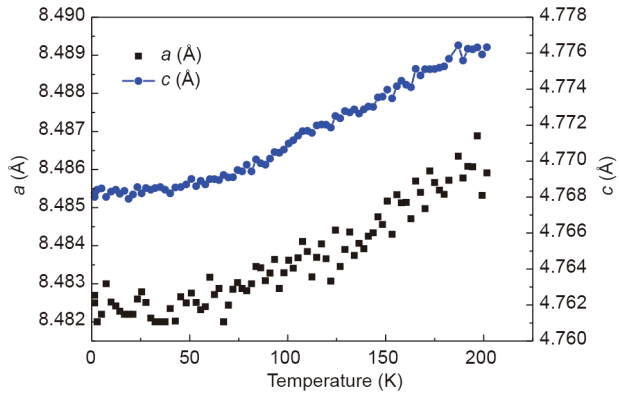

Fig. 5. Temperature dependence of the lattice parameters of $DyFe_{11}Ti$ in the temperature range of the two spin reorientation transitions.

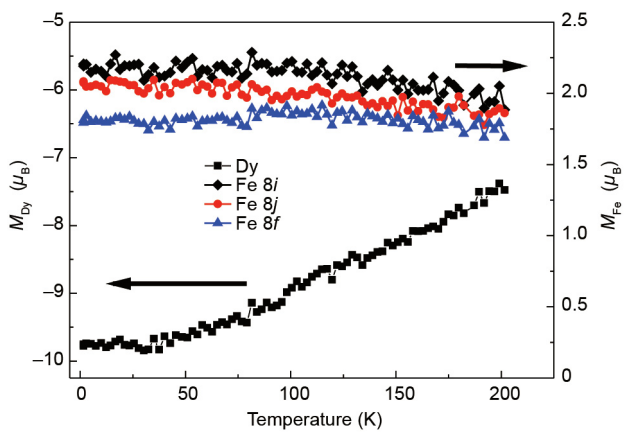

Fig. 6. Thermal evolution of the atomic magnetic moments, as derived from the Rietveld refinement of the neutron powder diffraction patterns recorded for $DyFe_{11}Ti$. M_{Dy}: magnetic moment of Dy; M_{Fe}: magnetic moment of Fe.

Table 2
Crystal structure parameters deduced from Rietveld refinement of the neutron powder diffraction data recorded for $DyFe_{11}Ti$ at 200 K.

Atom	Site	x/a	y/b	z/c	Occupancy (%)	$M(\mu_B)$
Dy	2a	0	0	0	100	−7.47(10)
Fe	8f	0.25	0.25	0.25	100	1.7(1)
Fe	8j	0.277(6)	0.5	0	100	1.86(7)
Fe/Ti	8i	0.358(9)	0	0	78/22	1.90(7)/0

$a = b = 8.486(6)$ Å; $c = 4.776(3)$ Å. x, y and z are the atomic position parameters. The angle of the magnetization direction with the c axis is 23°(2). The agreement factors are as follows: $R_B = 2.3\%$ and $R_{Mag} = 1.9\%$. M: magnetic moment.

in Ref. [14] and the ordering temperature of 552 K for the powder studied here. The shape of the experimental curve plotted in Fig. 4 is clearly very close to those discussed in Refs. [13,19] from theoretical and experimental perspectives, respectively. This finding favors the scenario of a first-order spin reorientation transition occurring gradually at T_{SR1}, and should resolve the controversy found in the literature. Our results are also in good agreement with the AC susceptibility results [14,19], which assigned a first-order type to the T_{SR1} and a second-order type to the spin reorientation at T_{SR2}. Indeed, a continuous variation of the magnetization typical of a second-order transition has been reported at T_{SR2} [19], leading to a divergence of the susceptibility at that temperature due to the vanishing anisotropy.

It is interesting to note that no anomaly occurred in the temperature dependence of the lattice parameters at either T_{SR1} or T_{SR2}. On the contrary, the two lattice parameters exhibited a normal behavior, being almost constant up to 50 K and then increasing as a result of thermal expansion, with a rate of 2.3×10^{-5} and 3.1×10^{-5} Å·K^{-1} for c and a, respectively (Fig. 5). The absence of any features on the lattice parameters may be surprising, but is in agreement with the normal thermal expansion reported earlier for $DyFe_{11}Ti$ [20]. In contrast, the magnetostriction has been found to be very sensitive to temperature changes in the vicinity of the spin reorientation phase transitions in single-crystal $DyFe_{11}Ti$ [21]. The magnitude of the atomic magnetic moments (Fig. 6) decreased upon increasing temperature, but did not seem to be influenced by the occurrence of spin reorientation at T_{SR1}. A very small evolution of the Fe magnetic moment was observed in the studied temperature range, which is in good agreement with the relatively large ordering temperature of $DyFe_{11}Ti$. The dysprosium magnetic moment was much more sensitive to temperature change and presented a quasi-linear dependence above 50 K, with a reduction rate of $0.0145\mu_B \cdot K^{-1}$.

4. Conclusions

Thanks to neutron diffraction analysis, the Ti content of $DyFe_{11}Ti$ was determined and the crystal structure was investigated. Ti atoms were found to be exclusively located on the 8i position. The magnetic structure of $DyFe_{11}Ti$ exhibits a basal plane anisotropy at 2 K with an alignment of the Dy and Fe magnetic moments within the basal plane; the easy magnetization axis is along the [110] direction. The lowest temperature spin reorientation manifests itself at 90 K by an abrupt decrease of the angle between the easy magnetization direction and the [001] direction. At this T_{SR1}, our experimental results favor the first-order spin reorientation transition scenario. A conical magnetic structure was observed in a wide temperature range above the basal plane anisotropy domain. Upon increasing the temperature further, the magnetic moments tilted toward the c axis, thus leading to the uniaxial character reported in the literature at 300 K. This transition from a conical magnetic structure to the easy plane occurred close to 200 K. A large temperature dependence of the Dy magnetic moment was observed, in contrast to the Fe moments, which remained almost identical in the studied temperature domain. A study of the thermal evolution of the lattice parameters did not present any anomalous behavior at the spin reorientation—a result that agrees with the earlier reported thermal expansion. Further studies are in progress to investigate the magnetic behavior of isotype $RFe_{11}Ti$ hydrides, and of $DyFe_{11}TiH$ in particular.

Acknowledgements

The use of the Collaborative Research Group instrument D1B operated by the CNRS at the ILL is warmly acknowledged, as well as the ILL for providing the neutron beam.

Compliance with ethics guidelines

Olivier Isnard and Eder J. Kinast declare that they have no conflict of interest or financial conflicts to disclose.

References

[1] Buschow KHJ. Permanent magnet materials based on tetragonal rare earth compounds of the type $RFe_{12-x}M_x$. J Magn Magn Mater 1991;100(1–3):79–89.
[2] Li HS, Coey JMD. Magnetic properties of ternary rare-earth transition-metal compounds. In: Buschow KHJ, editor. Handbook of magnetic materials, vol 6. Amsterdam: Elsevier; 1991.
[3] Buschow KHJ, editor. Electronic and magnetic properties of metals and ceramics, part II. In: Cahn RW, Haasen P, Kramer EJ, editors. Materials

science and technology—a comprehensive treatment, vol. 3B. Berlin: VCH Publishing; 1994.
[4] Isnard O, Miraglia S, Guillot M, Fruchart D. Hydrogen effects on the magnetic properties of $RFe_{11}Ti$ compounds. J Alloys Compd 1998;275–277:637–41.
[5] Nikitin SA, Tereshina IS, Verbetsky VN, Salamova AA. Transformations of magnetic phase diagram as a result of insertion of hydrogen and nitrogen atoms in crystalline lattice of $RFe_{11}Ti$ compounds. J Alloys Compd 2001;316(1–2):46–50.
[6] Florio JV, Rundle RE, Snow AI. Compounds of thorium with transition metals. I. the thorium-manganese system. Acta Crystallogr 1952;5(4):449–57.
[7] Isnard O, Guillot M. On the magnetic properties of $RFe_{11}TiH_x$ compounds. J Optoelectron Adv Mater 2008;10(4):744–9.
[8] Hu BP, Li HS, Coey JMD. Relationship between $ThMn_{12}$ and Th_2Ni_{17} structure types in the $YFe_{11-x}Ti_x$ alloy series. J Appl Phys 1990;67(9):4838–40.
[9] Hu BP, Li HS, Coey JMD, Gavigan JP. Magnetization of a $Dy(Fe_{11}Ti)$ single crystal. Phys Rev B Condens Matter 1990;41(4):2221–8.
[10] Andreev AV, Bartashevich MI, Kudrevatykh NV, Razgonyaev SM, Sigaev SS, Tarasov EN. Magnetic and magnetoelastic properties of $DyFe_{11}Ti$ single crystals. Phys B 1990;167(2):139–44.
[11] Tereshina IS, Telegina IV, Skokov KP. Investigation of spin-reorientation phase transitions in single-crystal $DyFe_{11}Ti$. Phys Solid State 1998;40(4):643–4.
[12] Piquer C, Isnard O, Grandjean F, Long GJ. Magnetic and Mössbauer spectral properties of $DyFe_{11}Ti$ and $DyFe_{11}TiH$. J Magn Magn Mater 2003;265(2):156–66.
[13] Kuz'min MD. On the gradual character of the first-order spin reorientation transition in $DyFe_{11}Ti$. J Appl Phys 2000;88(12):7217–22.
[14] Kuz'min MD, García LM, Artigas M, Bartolomé J. Ac susceptibility of a $DyFe_{11}Ti$ single crystal. Phys Rev B Condens Matter 1996;54(6):4093–100.
[15] Rodríguez-Carvajal J. Recent advances in magnetic structure determination by neutron powder diffraction. Phys B 1993;192(1–2):55–69.
[16] Isnard O, Fruchart D. Magnetism in Fe-based intermetallics: relationships between local environments and local magnetic moments. J Alloys Compd 1994;205(1–2):1–15.
[17] Piquer C, Grandjean F, Isnard O, Long GJ. An analysis of the hyperfine parameters of the $RFe_{11}Ti$ and $RFe_{11}TiH$ compounds, where R is a rare-earth element. J Phys Condens Matter 2006;18(1):205–19.
[18] Piquer C, Grandjean F, Isnard O, Long GJ. A phenomenological model for the rare-earth contribution to the magnetic anisotropy in $RFe_{11}Ti$ and $RFe_{11}TiH$. J Phys Condens Matter 2006;18(1):221–42.
[19] García LM, Bartolomé J, Algarabel PA, Ibarra MR, Kuz'min MD. Spontaneous and field induced spin reorientation transitions of $DyFe_{11}Ti$ single crystal. J Appl Phys 1993;73(10):5908–10.
[20] Zubenko VV, Tereshina IS, Telegina IV, Tereshina EA, Luchev DO, Pankratov NY. Specific features in thermal expansion of $RFe_{11}Ti$ single crystals. Phys Sol State 2001;43(7):1273–7.
[21] Nikitin SA, Tereshina IS, Pankratov NY. Magnetostriction in the vicinity of the spin-reorientation phase transitions in single crystal $DyFe_{11}Ti$. Phys Sol 1999;41(9):1508–10.